Inorg. Chem. **2007**, *46*, 3663–3668

Critical Role of Water Content in the Formation and Reactivity of Uranium, Neptunium, and Plutonium Iodates under Hydrothermal Conditions: Implications for the Oxidative Dissolution of Spent Nuclear Fuel

Travis H. Bray,[†] Jie Ling,[†] Eun Sang Choi,[‡] James S. Brooks,[‡] James V. Beitz,[§] Richard E. Sykora,[||] Richard G. Haire,[⊥] David M. Stanbury,[†] and Thomas E. Albrecht-Schmitt*,[†]

Department of Chemistry and Biochemistry and E. C. Leach Nuclear Science Center, Auburn University, Auburn, Alabama 36849, Department of Physics and National High Magnetic Field Laboratory, Florida State University, Tallahassee, Florida 32310, Chemistry Division, Argonne National Laboratory, Argonne, Illinois 60439, Department of Chemistry, University of South Alabama, Mobile, Alabama 36688, and Chemical Sciences Division, Transuranium Research Laboratory, Oak Ridge National Laboratory, MS 6375, Oak Ridge, Tennessee 37831

Received January 30, 2007

The reactions of $^{237}NpO_2$ with excess iodate under acidic hydrothermal conditions result in the isolation of the neptunium(IV), neptunium(V), and neptunium(VI) iodates, $Np(IO_3)_4$, $Np(IO_3)_4 \cdot nH_2O \cdot nHIO_3$, $NpO_2(IO_3)$, $NpO_2(IO_3)_2(H_2O)$, and $NpO_2(IO_3)_2 \cdot H_2O$, depending on both the pH and the amount of water present in the reactions. Reactions with less water and lower pH favor reduced products. Although the initial redox processes involved in the reactions between $^{237}NpO_2$ or $^{242}PuO_2$ and iodate are similar, the low solubility of $Pu(IO_3)_4$ dominates product formation in plutonium iodate reactions to a much greater extent than does $Np(IO_3)_4$ in the neptunium iodate system. UO_2 reacts with iodate under these conditions to yield uranium(VI) iodates solely. The isotypic structures of the actinide(IV) iodates, $An(IO_3)_4$ (An = Np, Pu), are reported and consist of one-dimensional chains of dodecahedral An(IV) cations bridged by iodate anions. The structure of $Np(IO_3)_4 \cdot nH_2O \cdot nHIO_3$ is constructed from NpO_9 tricapped-trigonal prisms that are bridged by iodate into a polar three-dimensional framework structure. Second-harmonic-generation measurements on a polycrystalline sample of the Th analogue of $Np(IO_3)_4 \cdot nH_2O \cdot nHIO_3$ reveal a response of approximately 12× that of α-SiO_2. Single-crystal magnetic susceptibility measurements of $Np(IO_3)_4$ show magnetically isolated Np(IV) ions.

Introduction

Under the oxidizing conditions present in the groundwater taken from wells near Yucca mountain, introduced iodine should occur in the form of both iodide, I^-, and iodate, IO_3^-.[1] Whereas I^- is not expected to form strong complexes with actinide ions in aqueous media,[2] IO_3^- forms stable, inner-sphere complexes with actinides.[3] The remarkable insolubility of actinide iodates has been used for decades to precipitate actinides selectively from fission products and other elements.[4] The initial forms of actinides in spent nuclear fuel (SNF) are primarily reduced, e.g., UO_2, NpO_2, and PuO_2. Owing to its high vapor pressure, iodine is expected to be

* To whom correspondence should be addressed. E-mail: albreth@auburn.edu.
[†] Auburn University.
[‡] Florida State University.
[§] Argonne National Laboratory.
[||] University of South Alabama.
[⊥] Oak Ridge National Laboratory.

(1) (a) Bruchertseifer, H.; Cripps, R.; Guentay, S.; Jaeckel, B. *Anal. Bioanal. Chem.* **2003**, *375*, 1107. (b) Huang, Z.; Ito, K.; Timerbaev, A. R.; Hirokawa, T. *Anal. Bioanal. Chem.* **2004**, *378*, 1836. (c) Bard, A. J.; Parsons, R.; Jordan, J. *Standard Potentials in Aqueous Solution*; Dekker: New York, 1985. (d) Charlot, G. *Oxidation-Reduction Potentials*: Pergamon: London, 1958. (e) Pourbaix, M. *Atlas d'equilibries electrochemiques à 25 °C*; Gautier Villars: Paris, 1963.

(2) (a) Crawford, M.-J.; Ellern, A.; Karaghiosoff, K.; Mayer, P. Noth, H.; Suter, M. *Inorg. Chem.* **2004**, *43*, 7120. (b) Berthet, J.-C.; Nierlich, M.; Ephritikhine, M. *Chem. Commun.* **2004**, *7*, 870.

(3) (a) Choppin, G. R.; Khalili, F. I.; Rizkalla, E. N. *J. Coord. Chem.* **1992**, *26*, 243. (b) Rao, P. R. V.; Patil, S. K. *Radiochem. Radioanal. Lett.* **1978**, *36*, 169.

(4) (a) Seaborg, G. T.; Wahl, A. C. *J. Am. Chem. Soc.* **1948**, *70*, 1128. (b) Cunningham, B. B.; Werner, L. B. *J. Am. Chem. Soc.* **1949**, *71*, 1521. (c) Seaborg, G. T.; Thompson, S. G. U.S. Patent 2,950,168, 1960.

10.1021/ic070170d CCC: $37.00
Published on Web 03/31/2007

concentrated near the surface and in grain boundaries in SNF where it could react with dissolved oxygen in water to form iodate.[5] Therefore, the products of the reactions of tetravalent actinides with iodate might play an important role in the potential release of several key long-lived radionuclides (e.g., ^{129}I, $t_{1/2} = 1 \times 10^7$ y (y = years); ^{238}U, $t_{1/2} = 4.46 \times 10^9$ y; ^{237}Np, $t_{1/2} = 2.14 \times 10^6$ y, and ^{239}Pu, $t_{1/2} = 2.411 \times 10^4$ y) into the environment in the event of aged SNF contacting groundwater. During the lifetime of stored SNF, it is possible that minute cracks and pores will form in the casings. This scenario will significantly limit the amount of groundwater interacting with the nuclear waste. Herein, we show that the chemistry that occurs under hydrothermal conditions where a limited amount of water is present can be different from what is predicted based on homogeneous solution redox potentials.[6]

Experimental Section

Syntheses. $Th(NO_3)_4 \cdot xH_2O$ (99%, Alfa Aesar), UO_2 (99.8%, Alfa Aesar, depleted), $^{237}NpO_2$ (99.9%, Oak Ridge, $t_{1/2} = 2.14 \times 10^6$ y), $^{242}PuO_2$ (99.9%, Oak Ridge, $t_{1/2} = 3.76 \times 10^5$ y), and HIO_3 (99.5%, Alfa Aesar) were used as received. Distilled and Millipore-filtered water with a resistance of 18.2 MΩ·cm was used in all reactions. Reactions were run in Parr 4749 autoclaves with custom-made 10 mL poly(tetrafluoroethylene) liners. All reactions were conducted with 10 mg of AnO_2 (An = U, Np, Pu) and a 10-fold molar amount of iodic acid unless otherwise noted. For the Th reactions, $Th(NO_3)_4 \cdot xH_2O$ was used as the starting material. Sealed reaction vessels were placed in box furnaces that had been preheated to 200 °C. The reactions occurred under an air atmosphere. Cooling was accomplished by turning the furnaces off. All solid products reported in the reaction schemes were isolated as single crystals and their structures determined using single-crystal X-ray diffraction to confirm their identity.

All studies were conducted in a laboratory dedicated to studies on transuranium elements. This laboratory is located in a nuclear science facility and is equipped with HEPA-filtered hoods and gloveboxes that are ported directly into the hoods. A series of counters continually monitor radiation levels in the laboratory. The laboratory is licensed by the state of Alabama (a NRC-compliant state) and Auburn University's Radiation Safety Office. All experiments were carried out with approved safety operating procedures. All free-flowing solids are worked with in the gloveboxes, and solid products are only examined when coated with either water or Krytox oil and water.

As a cautionary note, both $Np(IO_3)_4$ and $Pu(IO_3)_4$ are pleochroic owing to their low-dimensional structures. Different crystal growth conditions lead to changes in crystal morphology, agglomeration of crystallites, and different product coloration, depending on the angle with which the crystallites are viewed. For $Np(IO_3)_4$, gray to green to black transitions can be observed by rotating single crystals and clusters of crystals, whereas for $Pu(IO_3)_4$, blue to green to brown coloration is exhibited. Crystals of $Np(IO_3)_4 \cdot nH_2O \cdot nHIO_3$ have a very pale yellow coloration. Crystals of $Th(IO_3)_4 \cdot nH_2O \cdot nHIO_3$ are colorless.

Table 1. Crystallographic Data for $Np(IO_3)_4$, $Pu(IO_3)_4$, and $Np(IO_3)_4 \cdot nH_2O \cdot nHIO_3$

	formula		
	$Np(IO_3)_4$	$Pu(IO_3)_4$	$Np(IO_3)_4 \cdot nH_2O \cdot nHIO_3$
formula mass (amu)	936.60	941.60	956.41
cryst syst	tetragonal	tetragonal	rhombohedral
space group	$P4_2/n$ (No. 86)	$P4_2/n$ (No. 86)	$R3c$
a (Å)	9.8790(5)	9.869(1)	21.868(1)
c (Å)	5.3063(4)	5.2861(7)	12.9705(8)
V (Å^3)	517.87(5)	514.8(1)	5371.4(5)
Z	2	2	18
T (°C)	−80	−80	−80
λ (Å)	0.71073	0.71073	0.71073
ρ_{calcd} (g cm^{-3})	6.006	6.074	5.322
μ(Mo Kα) (cm^{-1})	220.17	184.57	191.93
$R(F)$ for $F_o^2 > 2\sigma(F_o^2)$[a]	0.0250	0.0266	0.0403
$R_w(F_o^2)$[b]	0.0654	0.0467	0.0880

[a] $R(F) = \sum||F_o| - |F_c||/\sum|F_o|$. [b] $R_w(F_o^2) = [\sum[w(F_o^2 - F_c^2)^2]/\sum wF_o^4]^{1/2}$.

Crystallographic Studies. Single crystals of $An(IO_3)_4$ (An = Np, Pu) and $Np(IO_3)_4 \cdot nH_2O \cdot nHIO_3$ were optically aligned on a Bruker SMART APEX CCD X-ray diffractometer. For each crystal, intensity measurements were performed using graphite-monochromated Mo Kα radiation from a sealed tube and a monocapillary collimator. SMART was used for preliminary determination of the cell constants and data collection control. The intensities of the reflections of a sphere were collected by a combination of three sets of exposures (frames). Each set had a different ϕ angle for the crystal, and each exposure covered a range of 0.3° in ω. A total of 1800 frames were collected.

The determination of integrated intensities and global cell refinement was performed with the Bruker *SAINT* (v 6.02) software package using a narrow-frame integration algorithm. Numerical and semiempirical absorption corrections were applied to the data.[7] The program suite *SHELXTL* (v 5.1) was used for space group determination, structure solution, and refinement.[8] The final refinement included anisotropic displacement parameters for all atoms. Some crystallographic details are listed in Table 1 for $An(IO_3)_4$ (An = Np, Pu) and $Np(IO_3)_4 \cdot nH_2O \cdot nHIO_3$; additional details can be found in the Supporting Information.

Magnetic Susceptibility Measurements. Magnetism data for $Np(IO_3)_4$ were measured with a Quantum Design MPMS 7 T magnetometer/susceptometer between 2 and 300 K and in applied fields of up to 7 T. Direct-current temperature-dependent susceptibility measurements were made under zero-field-cooled conditions with an applied field of 0.1 T. Susceptibility values were corrected for the sample diamagnetic contribution according to Pascal's constants,[9] as well as for the sample holder diamagnetism. Two different single-crystal samples (0.76 and 0.44 mg) were used for the susceptibility measurement. The data shown here are from the larger sample, which gave results identical with those of the smaller sample. The sample was cooled down at zero field, and the magnetic moment was measured at fixed field. The Curie constant was obtained either from the Curie-Weiss fitting or from the slope of $(\chi - \chi_0)^{-1}$ vs temperature, which gave similar results.

(5) Kaholek, M.; Triendl, L. *React. Kinet. Catal. Lett.* **1998**, *63*, 297.
(6) (a) Morss, L. R.; Edelstein, N. M.; Fuger, J. *The Chemistry of the Actinide and Transactinide Elements*; Springer: Heidelberg, 2006; Vol. 2, Chapter 6. (b) Katz, J. J.; Seaborg, G. T.; Morss, L. R. *The Chemistry of the Actinide Elements*, 2nd ed.; Chapman and Hall: New York, 1986; Vol. 1, Chapter 6.
(7) Sheldrick, G. M. *SADABS* 2001, Program for Absorption Correction Using SMART CCD Based on the Method of Blessing: Blessing, R. H. *Acta Crystallogr.* **1995**, *A51*, 33.
(8) Sheldrick, G. M. *SHELXTL PC*, version 6.12, An Integrated System for Solving, Refining, and Displaying Crystal Structures from Diffraction Data; Siemens Analytical X-ray Instruments, Inc.: Madison, WI, 2001.
(9) Mulay, L. N.; Boudreaux, E. A. *Theory and Applications of Molecular Diamagnetism*; Wiley-Interscience: New York, 1976.

Scheme 1

$$5NpO_2 + 12H^+ + 2IO_3^- \xrightarrow[H_2O]{200\ ^\circ C,\ 3\ days} 5NpO_2^{2+} + I_2 + 6H_2O \quad (1)$$

$$2NpO_2^{2+} + 4H^+ \xrightarrow[<375\ \mu L\ of\ H_2O]{200\ ^\circ C,\ 3\ days} 2Np^{4+} + 2H_2O + O_2 \quad (2)$$

$$Np^{4+} + 4IO_3^- \xrightarrow[100\ \mu L\ of\ H_2O]{200\ ^\circ C,\ 3\ days} Np(IO_3)_4 \quad (3)$$

$$2Np^{4+} + 8IO_3^- + nH_2O \xrightarrow[250\ \mu L\ of\ H_2O]{200\ ^\circ C,\ 3\ days} Np(IO_3)_4 + Np(IO_3)_4 \cdot nH_2O \quad (4)$$

$$NpO_2^{2+} + Np^{4+} + 2IO_3^- + 2H_2O \xrightarrow[375\ \mu L\ of\ H_2O]{200\ ^\circ C,\ 3\ days} 2NpO_2(IO_3) + 4H^+ \quad (5)$$

$$2NpO_2^{2+} + 4IO_3^- + 2H_2O \xrightarrow[500\ \mu L\ of\ H_2O]{200\ ^\circ C,\ 3\ days} NpO_2(IO_3)_2 \cdot H_2O + NpO_2(IO_3)_2(H_2O) \quad (6)$$

Nonlinear Optical Measurements. Powder second-harmonic-generation (SHG) measurements were performed on a Kurtz−Perry nonlinear optical system,[10] as modified by Porter and co-workers,[11] and updated here to include laser-pulse energy normalization. A Q-switched Nd:YAG laser (Continuum Surelite I-10), operated at 10 Hz, provided the 1064 nm light used for all measurements. The SHG intensity was recorded from $Th(IO_3)_4 \cdot nH_2O \cdot nHIO_3$ and from fine-ground α-quartz. These powders were placed in separate glass tubes of the same dimensions. No index of refraction matching fluid was used in these experiments. The SHG light at 532 nm was collected in reflection, selected by a narrow band-pass interference filter (Pomfret), and detected by a photomultiplier tube (RCA 1P28). A near-normal incidence beam splitter reflected a small fraction of the laser beam onto a pyroelectric detector (Molectron J3-05) that was used as a laser-pulse energy monitor. A digital storage oscilloscope (Tektronix TDS 640A) signal averaged and recorded both the SHG and incident laser-energy signals. The average laser power was measured separately with a calibrated Scientech volume-absorber calorimeter. The observed SHG intensity per unit laser intensity, $I^{2\omega}$, was obtained by dividing the SHG signal by the laser-energy signal. Replicate measurements determined the value of interest for the sample compound, $I^{2\omega}$ (s), and for α-quartz, $I^{2\omega}$ (q). The ratio of these values, $I^{2\omega}(s)/I^{2\omega}(q)$, was found to be 12 at an incident laser intensity of 6.7 MW/cm^2.

Results and Discussion

Reactions. When $^{237}NpO_2$ is reacted with excess iodate under acidic mild hydrothermal conditions, neptunium(IV), neptunium(V), and neptunium(VI) iodates are isolated as shown in Scheme 1.

Reaction 1 describes the direct two-electron oxidation of Np^{4+} to NpO_2^{2+} by iodate. Acidic dissolution of NpO_2 in the presence of oxygen typically yields Np(V) in the form of NpO_2^+ in solution (e.g., in 1 M HCl). Reaction 1 is governed by the strong oxidizing potential of iodate under acidic conditions that is sufficient to directly oxidize Np^{4+} to NpO_2^{2+}.[6] The formal potentials for these reactions are given below in Scheme 2.[6,12]

Scheme 2

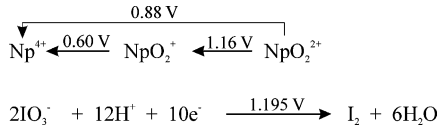

It is important to note that these $E°$ values are given at 25 °C and 1 atm. Our reactions are occurring at 200 °C and approximately 17 atm (if H_2O exhibits the vapor pressure of pure water), and therefore, these potentials can only be used for guidance. These reactions should be thought of as taking place in steam under autogenously generated pressure. There is approximately 170 μL of liquid water present at 200 °C in a reaction that starts with 250 μL of water. In contrast, there will only be 20 μL of liquid water present at 200 °C in a reaction that begins with 100 μL of water. When the reactions occur with only a limited amount of liquid water present, as demonstrated in reactions 2 and 7, reduction of NpO_2^{2+} back to Np^{4+} takes place.

$$2H^+ + NpO_2(IO_3)_2 \cdot H_2O + 2IO_3^- \xrightarrow[250\ \mu L\ of\ H_2O]{200\ ^\circ C,\ 3\ days} Np(IO_3)_4 + 2H_2O + {}^1/_2O_2 \quad (7)$$

When sufficient amounts of water are present to approximate a solution (500 μL), as in reaction 6, the predicted reaction between NpO_2 and iodate occurs, via reaction 1, and $NpO_2(IO_3)_2(H_2O)$ and $NpO_2(IO_3)_2 \cdot H_2O$ form.[13] Reaction 5 is the most interesting of this series and represents conditions under which comproportionation of Np^{4+} and NpO_2^{2+} occurs to yield 2 equiv of NpO_2^+. It is important to note that, even when the Np(VI) products are isolated as solids, they can be slowly converted to neptunium(IV) iodates by the application of appropriate hydrothermal conditions (250 μL of water), as shown in reaction 7. If the amount of water is increased to 500 μL, reduction does not take place.

Reactions 2−4 are not solely driven by the solution-phase thermodynamics of the oxidation of Np^{4+} by iodate but also by the reduction of Np(VI) to yield Np(IV) and the subsequent crystallization of the neptunium(IV) iodate

(10) Kurtz, S. K.; Perry, T. T. *J. Appl. Phys.* **1968**, *39*, 3798.
(11) Porter, Y.; Ok, K. M.; Bhuvanesh, N. S. P.; Halasyamani, P. S. *Chem. Mater.* **2001**, *13* 1910.
(12) Lide, D. R. *CRC Handbook of Chemistry and Physics*, 71st ed.; CRC Press: Boston, 1990; pp 8−18.
(13) Bean, A. C.; Scott, B. L.; Albrecht-Schmitt, T. E.; Runde, W. *Inorg. Chem.* **2003**, *42*, 5632.

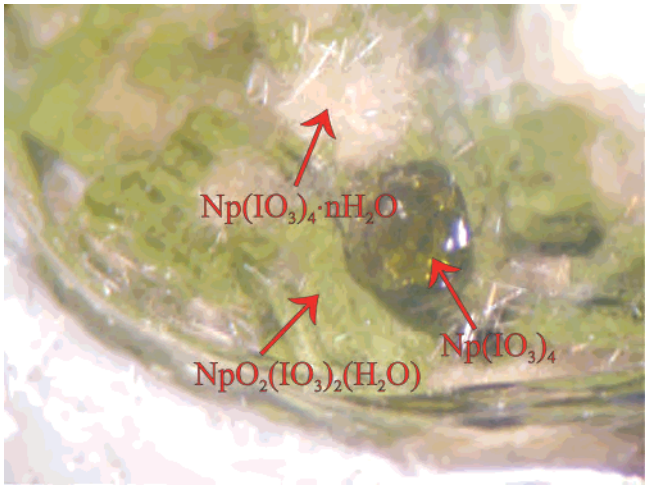

Figure 1. Photograph showing the hydrothermal reduction of the neptunium(VI) iodate $NpO_2(IO_3)_2(H_2O)$ to the neptunium(IV) iodates $Np(IO_3)_4$ and $Np(IO_3)_4{\cdot}nH_2O{\cdot}nHIO_3$.

products, $Np(IO_3)_4$ and $Np(IO_3)_4{\cdot}nH_2O{\cdot}nHIO_3$. Figure 1 depicts the results of reaction 7 and shows crystals of $Np(IO_3)_4$ and $Np(IO_3)_4{\cdot}nH_2O{\cdot}nHIO_3$ that have grown directly off the surface of the delaminating crystals of $NpO_2(IO_3)_2(H_2O)$. This result supports the hypothesis that the reaction is a solid-to-solid transformation that is probably surface-mediated. The same may be true for reactions 2−5. In the presence of a large external radiation source, radiolysis products of water (e.g., H, HO_2, and H_2O_2) might play a role in the reduction of Np(VI) to Np(IV).[14]

As was observed with Np, the reaction of PuO_2 with iodate leads to the two-electron oxidation of Pu^{4+} to PuO_2^{2+} with concomitant production of elemental iodine (reaction 8). In

Scheme 3

$$5PuO_2 + 12H^+ + 2IO_3^- \xrightarrow[H_2O]{200\ ^\circ C,\ 3\ days} 5PuO_2^{2+} + I_2 + 6H_2O \quad (8)$$

$$Pu^{4+} + 4IO_3^- \xrightarrow[100-1000\ \mu L\ of\ H_2O]{200\ ^\circ C,\ 3\ days} Pu(IO_3)_4 \quad (9)$$

contrast to the $^{237}NpO_2$ reactions, the reaction of $^{242}PuO_2$ with iodate with up to 1000 μL of water led to the formation of $Pu(IO_3)_4$ (reaction 9). These results imply that the hydrothermal chemistry of plutonium iodates is dominated to an even greater extent than in the Np reactions by the solubility-driven formation of the actinide(IV) iodates.

In previous work, it was shown that stock solutions of Pu^{4+} and NpO_2^+ react with excess metaperiodate, IO_4^-, to yield products that contain the actinides in the 6+ oxidation state (e.g., $NpO_2(IO_3)_2(H_2O)$ and $AnO_2(IO_3)_2{\cdot}H_2O$ (An = Np, Pu)).[13,15] Metaperiodate contains I(VII) and is a much stronger oxidant than iodate (1.601 vs 1.195 V). Clearly, the reactions reported herein of AnO_2 (An = Np, Pu) with iodate under hydrothermal conditions with limited amounts of water are dramatically different from those of aqueous actinide ions with very strong oxidants. Although these reactions are occurring at a much lower pH than natural groundwaters, this work calls into question the use of standard solution reactivity data on actinide ions to predict the behavior of SNF that will start off as a reduced solid. The thermodynamic data for actinide complexation are already being reevaluated in light of the substantial changes that occur at elevated temperatures.[16]

The least complex of these reactions is that of UO_2 with iodate. The process proceeds in accordance with Scheme 4, yielding only U(VI) iodates, such as $UO_2(IO_3)_2$ and $UO_2(IO_3)_2(H_2O)$.[17] Given the ease of oxidation of U^{4+} to UO_2^{2+}, this result is not surprising ($E^\circ = -0.327$ V).[6]

Scheme 4

$$5UO_2 + 12H^+ + 2IO_3^- \xrightarrow[H_2O]{200\ ^\circ C,\ 3\ days} 5UO_2^{2+} + I_2 + 6H_2O \quad (10)$$

$$2UO_2^{2+} + 4IO_3^- + H_2O \xrightarrow[H_2O]{200\ ^\circ C,\ 3\ days} UO_2(IO_3)_2(H_2O) + UO_2(IO_3)_2 \quad (11)$$

Structure of $An(IO_3)_4$ (An = Np, Pu). In addition to the new actinide reactivity patterns, these syntheses provide access to single crystals of $An(IO_3)_4$ (An = Np, Pu) and $Np(IO_3)_4{\cdot}nH_2O{\cdot}nHIO_3$. The crystal structure of $An(IO_3)_4$ (An = Np, Pu) consists of eight-coordinate, trigonal dodecahedral An(IV) centers (D_{2d}) bridged by iodate to form one-dimensional chains as shown in Figure 2a. These compounds are isostructural with $Ce(IO_3)_4$.[18] The Np centers reside on $\bar{4}$ sites, yielding two independent An−O bond distances of 2.329(4) Å (×4) and 2.358(4) Å (×4) (for $Np(IO_3)_4$). The I−O bond distances of 1.782(5), 1.811(4), and 1.827(4) Å are normal.[17] The terminal I−O bond distance is slightly shorter than those bridging to the Np(IV) ions. These chains pack together in a pinwheel fashion (Figure 2b). Although the structures of neptunium(IV) iodates are expected to be similar, if not identical, with those of thorium(IV), we have yet to isolate a thorium analogue of $An(IO_3)_4$ (An = Np, Pu), although the Ce(IV) version has been prepared, underscoring some of the problems of using early, less-radioactive actinides like Th(IV) and U(IV) as surrogates for Np(IV) and Pu(IV).[20] This was also observed in the An(VI) iodates, where the U(VI) and Pu(VI) compounds are not isostructural.[13,15,17]

(14) Vladimirova, M. V. *Radiochemistry* **1997**, *39*, 250.
(15) Runde, W.; Bean, A. C.; Albrecht-Schmitt, T. E.; Scott, B. L. *Chem. Commun.* **2003**, *4*, 478.
(16) Rao, L.; Srinivasan, T. G.; Garnov, A. Y.; Zanonato, P. L.; Di Bernardo, P.; Bismondo, A. *Geochim. Cosmochim. Acta* **2004**, *68*, 4821.
(17) (a) Weigel, F.; Engelhardt, L. W. H. *J. Less-Common Met.* **1983**, *91*, 339. (b) Bean, A. C.; Peper, S. M.; Albrecht-Schmitt, T. E. *Chem. Mater.* **2001**, *13*, 1266.
(18) (a) Staritsky, E.; Cromer, D. T. *Anal. Chem.* **1956**, *28*, 913. (b) Cromer, T.; Larson, A. C. *Acta Crystallogr.* **1956**, *9*, 1015.
(19) (a) Sullens, T. A.; Almond, P. M.; Albrecht-Schmitt, T. E. *Mater. Res. Soc.* **2006**, *893*, 283. (b) Gorden, A. E. V.; Shuh, D. K.; Tiedemann, B. E. F.; Wilson, R. E.; Xu, J.; Raymond, K. N. *Chem.—Eur. J.* **2005**, *11*, 2842.
(20) A historical footnote is worthwhile here: The microscale precipitation of $Pu(IO_3)_4$ was used by B. B. Cunningham and L. B. Werner to show, for the first time, that Pu has a stable 4+ oxidation state in 1942 (*4b*). Since this time, $Pu(IO_3)_4$ has been used as a benchmark compound because of its remarkable insolubility in low pH media. The structure, precise elemental analyses, and spectroscopic data for plutonium(IV) iodates have never been reported in the primary literature.

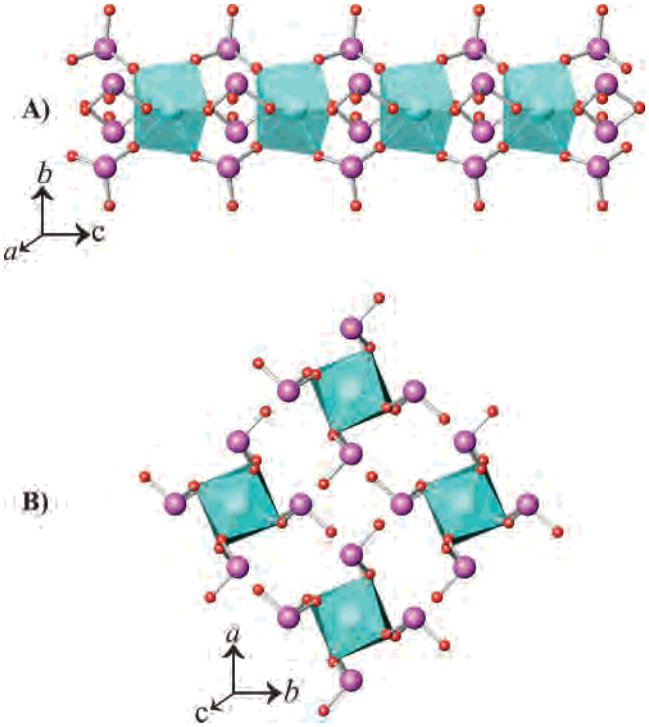

Figure 2. (a) View of the one-dimensional chains in $An(IO_3)_4$ (An = Np, Pu) consisting of eight-coordinate, dodecahedral An(IV) centers bridged by iodate. (b) Depiction of the pinwheel packing of the $An(IO_3)_4$ chains.

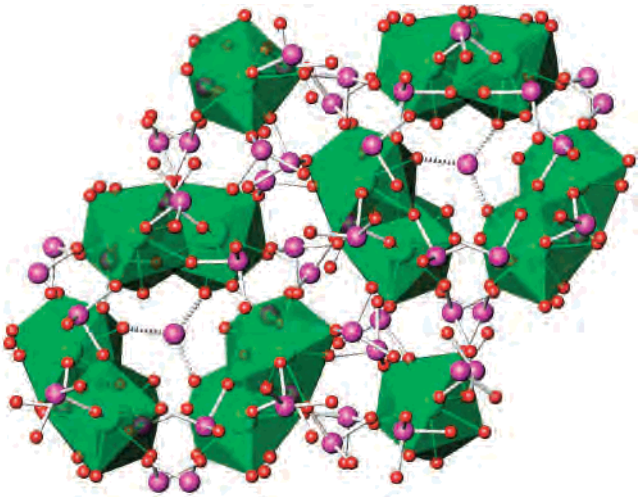

Figure 3. Depiction of the structure of $Np(IO_3)_4{\cdot}nH_2O{\cdot}nHIO_3$. This structure consists of a three-dimensional network constructed from nine-coordinate tricapped trigonal prismatic Np(IV) that are bridged by iodate anions to create the channels that extend along the *c* axis. The channels are partially filled by iodate anions or water molecules.

Structure of $Np(IO_3)_4{\cdot}nH_2O{\cdot}nHIO_3$. The structure of $Np(IO_3)_4{\cdot}nH_2O{\cdot}nHIO_3$ is similar to that of $K_3Am_3(IO_3)_{12}{\cdot}HIO_3$.[21] This structure type consists of a three-dimensional network constructed from nine-coordinate tricapped trigonal prismatic An(III) or An(IV) centers bridged by iodate anions to create a channel structure, as shown in Figure 3. The channels are partially filled by iodate anions or water molecules. Although the structure of $K_3Am_3(IO_3)_{12}{\cdot}HIO_3$ was reported as being stoichiometric, refinement on the occupancy of the iodate units in the channels reveals that they are only partially occupied. Furthermore, there are three very long I−O bonds of ca. 1.9 Å to this partially occupied iodine atom. We have prepared the Ce analogue of $K_3Am_3(IO_3)_{12}{\cdot}HIO_3$, and it shows partial occupancy of the iodine atoms in the channels, disorder and partial occupancy of the K^+ sites, and mixed valency (Ce(III)/Ce(IV)). Clearly, something unusual is taking place in this series of compounds associated with the iodate groups in the channels.

(21) Runde, W.; Bean, A. C.; Scott, B. L. *Chem. Commun.* **2003**, *15*, 1848.

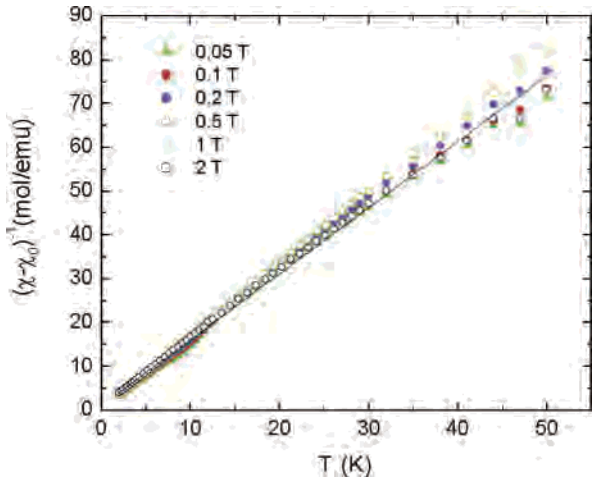

Figure 4. Temperature dependence of the inverse magnetic susceptibility of a $Np(IO_3)_4$ single crystal. The Curie−Weiss fitting curve is shown as a solid line.

$K_3Am_3(IO_3)_{12}{\cdot}HIO_3$ is reported as crystallizing in the polar rhombohedral space group *R*3*c*. Confirmation of the polarity of the space group via some external measurement, e.g., second-harmonic generation, is quite challenging given the extreme radioactivity of ^{241}Am. Although ^{237}Np is substantially less radioactive than ^{241}Am, it nevertheless poises serious handling challenges. Fortunately, as the result of separate studies, the Th analogue of $Np(IO_3)_4{\cdot}nH_2O{\cdot}nHIO_3$ was prepared, and second-harmonic-generation measurements were performed that showed a response of approximately 12× that of α-quartz, confirming the acentricity of the structure.

An unusual type of disorder to explain the abnormal bond distances and partial occupancy in this family of compounds is proposed here based on the following data: (1) The ninth capping position (O(13)) around the NpO_9 units appears to be fully occupied. (2) The atom lying at the center of the channels refines best as a partially occupied iodine. (3) The displacement parameters for O(13) are large (all light atoms were refined isotropically in $K_3Am_3(IO_3)_{12}{\cdot}HIO_3$). Taken together, a model can be proposed where the channels are occupied either by iodate or only by the capping water molecules. This would create an oxygen position (O(13)) that is an average of the water position(s) and the position(s) of the oxygen atoms from the iodate unit.

The Np−O bond distances range from 2.296(13) to 2.68(2) Å; the longest distance is to the coordinating water molecules in the channels. The four ordered iodate anions that are a part of the three-dimensional network contain regular I−O bond distances that range from 1.781(12) to 1.827(13) Å. All other aspects of the structure are also normal.

Magnetic Properties of $Np(IO_3)_4$. $Np(IO_3)_4$ crystallizes as single crystals that can have maximum dimensions as large as several millimeters, making this compound amenable to single-crystal magnetic susceptibility measurements. Magnetic susceptibility data for $Np(IO_3)_4$ are shown in Figure 4. Data were collected on two different crystals, yielding μ_{eff} of 2.22 and 2.25 μ_B per Np atom for the different crystals. The observed magnetic moment for the Np^{4+} ions in $Np(IO_3)_4$ is markedly lower than that calculated for the free ions (3.62 μ_B).[22] This is not a reflection of the covalency of the 5f orbitals but rather arises from the crystal field effects in $Np(IO_3)_4$,[23] as has also been suggested recently for two Np(V) compounds.[24] Magnetic fields well outside of the range of a standard 7 T magnet would be needed to achieve full saturation of the magnetic moment.[23] The data follow the Curie−Weiss law with $\theta = 0.0(5)$ K, indicating that the Np(IV) ions are magnetically isolated from one another. This observation is consistent with the large Np···Np distance of 5.306(1) Å within the one-dimensional chains.

Conclusions

These synthetic, structural, and magnetic data provide new avenues for addressing the reactivity, structures, and properties of transuranic compounds. The use of hydrothermal conditions with smaller amounts of water than has typically been employed gives access to pure compounds in the form of single crystals that have not been previously available from standard synthetic techniques. In a general sense, the actinide chemistry presented here can be considered as being a part of a larger synthetic methodology wherein redox reactions are used to control the introduction of ions that lead to the slow crystallization of highly insoluble products.[25] This gradual introduction of reactants facilitates crystal growth of compounds that normally only form microcrystalline or amorphous powders.

Acknowledgment. We are grateful for support provided by the Office of Civilian Radioactive Waste Management, Office of Science and Technology and International, through a subcontract with Argonne National Laboratory, and by the Chemical Sciences, Geosciences, and Biosciences Division, Office of Basic Energy Sciences, Office of Science, Heavy Elements Program, U.S. Department of Energy, under Grant DE-FG02-01ER15187, and under Contract DE-AC02-06CH11357 at Argonne National Laboratory and Contract DE-AC05-00OR22725 with Oak Ridge National Laboratory, managed by UT-Battelle, LLC. J.S.B. and E.-S.C. acknowledge support from NSF-DMR 0203532. A portion of this work was performed at the National High Magnetic Field Laboratory, which is supported by the National Science Foundation Cooperative Agreement No. DMR-0084173, the State of Florida, and the Department of Energy.

Supporting Information Available: X-ray crystallographic files for $Np(IO_3)_4$, $Pu(IO_3)_4$, and $Np(IO_3)_4 \cdot nH_2O \cdot nHIO_3$ in CIF format. This material is available free of charge via the Internet at http://pubs.acs.org.

IC070170D

(22) Kittel, C. *Introduction to Solid State Physics*, 6th ed.; Wiley: New York, 1986.
(23) (a) Morss, L. R.; Edelstein, N. M.; Fuger, J. *The Chemistry of the Actinide and Transactinide Elements*; Springer: Heidelberg, 2006; Vol. 4, Chapter 20.
(24) Forbes, T. Z.; Burns, P. C.; Soderholm, L.; Skanthakumar, S. *Chem. Mater.* **2006**, *18*, 1643.
(25) See, for example: Grohol, D.; Matan, K.; Cho, J.-H.; Lee, S.-H.; Lynn, J. W.; Nocera, D. G.; Lee, Y. S. *Nat. Mater.* **2005**, *4*, 323.